



Trade Science Inc.

ISSN : 0974 - 7486

Volume 8 Issue 2

# Materials Science

An Indian Journal

Full Paper

MSAIJ, 8(2), 2012 [73-79]

## Structural changes of Al-6%Ti alloy after hot extrusion and elevated temperature creep

Al-Badrawy A.Abo El-Nasr<sup>1</sup>, Mohamed Ayad<sup>2\*</sup>

<sup>1</sup>Department of Mechanical Engineering, College of Engineering, Qassim University, Buraidah, (KSA)

<sup>2</sup>Department of Mechanical Engineering, College of Engineering, Taif University, Taif, (KSA)

E-mail : ayadmoh2003@yahoo.com; albadrawy@qec.edu.sa

Received: 5<sup>th</sup> August, 2011 ; Accepted: 5<sup>th</sup> September, 2011

### ABSTRACT

This paper presents some new findings related to the structural changes of Al-6wt%Ti alloy after hot extrusion and elevated temperature creep. This alloy was fabricated by ingot metallurgy (IM) followed by hot extrusion processes, annealed at 650 °C for 48 hrs and then subjected to elevated temperature creep tests at 590 and 620 °C. Double shear specimen configuration was used in the creep tests due to its suitability for deformation analysis. Microstructure changes of the alloy under these processes were examined and analyzed in terms of size and aspect ratio of the second phase, Al<sub>3</sub>Ti intermetallic compound, by using the optical microscopy and image analysis facility. The results of this work showed the an improvement in size and redistribution of Al<sub>3</sub>Ti intermetallic compound after hot extrusion and creep tests. The application of such processes reduced the size and aspect ratio of the large flaky shape Al<sub>3</sub>Ti particles to uniformly distributed smaller particles. The creep curves of this alloy have been dominated by the primary creep stage followed by very short steady state stage and no indication of the existence of the tertiary creep stage. The analysis of this improvement was discussed in terms of the particle size and aspect ratio of Al<sub>3</sub>Ti compound.

© 2012 Trade Science Inc. - INDIA

### KEYWORDS

Structural change;  
Al-6%Ti alloy;  
Al<sub>3</sub>Ti intermetallic compound;  
Creep;  
Aspect ratio.

### INTRODUCTION

Aluminum alloys reinforced with ceramic particles are attractive for applications requiring higher stiffness and strength than traditional aluminum alloys. The general principle associated with these types of materials is to combine the matrix properties, i.e., ductility, fracture toughness and machineability, with reinforcement properties, i.e., stiffness, strength and thermal stability. It has been frequently reported, experimentally, that the in-

corporation of ceramic reinforcements into metallic matrices results in significant changes in the microstructure of the matrix material<sup>[1,2]</sup>. These changes include elevated dislocation densities, refined matrix grain size and reinforcement and enhanced precipitation kinetics<sup>[3,4]</sup>.

Al-Ti based alloys are now extensively used in high temperature structural applications due to the existence of highly stable Al<sub>3</sub>Ti phase and very low equilibrium solubility and diffusivity of Ti in Al<sup>[5]</sup>. Since the Al-rich intermetallic compound Al<sub>3</sub>Ti has a low density (3.3 g/

## Full Paper

cm<sup>3</sup>), a relatively high melting point (1350 °C) and high elastic modulus (166 GPa)<sup>[1]</sup>, titanium has been selected as the preferred alloying element. These alloys have been shown to exhibit attractive combinations of low density (~2.8 g/cm<sup>3</sup>), high modulus, elevated temperature strength, thermal stability, and corrosion resistance<sup>[2-6]</sup>. There have been many efforts to improve the mechanical behavior of Al-Ti alloys at high temperature by alloying elements addition, microstructure refinement, and heat treatment<sup>[1,2]</sup>. Results of dynamic modulus measurements showed that an increase of ~2.5 GPa in the modulus is obtained for every 1 wt% Ti present in the alloy<sup>[5]</sup>. Microstructure refinement of such alloys has been extensively investigated because initial structures of alloys have a significant influence on the mechanical and physical properties of finished products<sup>[4-11]</sup>. The finer grain and particle size reduce the size of defects such as microporosity, producing improved mechanical properties. Problems with Al-Ti master alloys can also be agglomeration of the carbides and blockage of defects during subsequent forming operations.

Al-Ti alloys are characterized by fine size and large volume fraction of fine dispersions of Al<sub>3</sub>Ti, Al<sub>4</sub>C<sub>3</sub> and Al<sub>2</sub>O<sub>3</sub> particles<sup>[8,9]</sup>. The contribution of each constituent to the strength of Al-Ti alloys has been suggested by Merchandani et al.<sup>[6]</sup>; the high temperature strength is strongly controlled by the carbide and oxide dispersoids. Al<sub>3</sub>Ti compound on the other hand contribute strongly to the stiffness and strength of these alloys, and appear to be responsible for improving the high temperature ductility of such alloys. It is found in the literature that no systematic information have been reported for the after-fabrication treatment on the features of Al<sub>3</sub>Ti intermetallic compound.

In this work, Al-6wt.% Ti alloy was fabricated by ingot metallurgy technique, hot extruded, annealed and then subjected to elevated temperature-low stress creep tests. The effect of these processes on the features and scale of Al<sub>3</sub>Ti compound in terms of its size and aspect ratio was studied. All these structural changes of the present alloy were digitally analyzed and discussed.

## EXPERIMENTAL

### Materials

The material used in this work was Al-Ti alloy (6

wt.% Ti) manufactured by ingot metallurgy (IM) technique. A charge of pure Al metal (99.5%) with 6 wt.% Ti (99% minimum) was melted and mechanically stirred in a graphite crucible heated by an electric resistance furnace up to 720±3 °C, holding 20 min at the temperature, then the melt was directly poured into the mold. The chemical composition (in wt.%) of the obtained cast was ; 6.10% Ti, 0.18% Fe, 0.13% O and the balance was Aluminum. The cast material is hot extruded through a cylindrical die with an extrusion ratio 4:1 at 450 °C to ~9 mm diameter rod.

### Mechanical testing

Fully rounded double shear test specimens were cut from the as-extruded rod parallel to the extrusion axis. Creep tests were conducted using double shear specimens with 6.4 mm gauge diameter and 34.9 mm total length. Prior creep testes, the specimens were annealed in air at 650 °C for 48 hr. This procedure was performed in order to stabilize the internal structure of the material. The specimens were stressed under constant load condition normal to the extrusion direction using a (SATEC testing machine). Due to double shear configuration<sup>[12]</sup>, constant load implies constant stress. Extra details regarding the tests, specimen's configuration and measurements are found elsewhere<sup>[13]</sup>. Figure 1 shows a photograph of the testing machine used in the present work. The creep data was obtained by conducting a series of creep tests on identical specimens at testing temperatures, 590 °C (863 K) and 620 °C (893 K) under stresses ranged from 1 MPa to 7 MPa. These elevated temperature tests were chosen in order to help



Figure 1 : Universal testing machine used in this work.

in the material flow during the creep deformation.

### Microstructure investigation

For microstructure analysis, the specimens were sectioned parallel to the extrusion axis, ground, polished, etched, and then examined using an optical microscope. Samples from the as-cast, extruded and crept materials were examined for characterizing the microstructure features and scale. Moreover, the features of the Al<sub>3</sub>Ti compound were digitized and statistically analyzed using image analysis facility.

## RESULTS AND DISCUSSION

### Creep behavior

A typical example of creep curve of Al-6wt.% Ti specimen, tested under 1 MPa in shear at 620 °C, is shown in Figure 2. As seen, the creep curve exhibits extensive primary creep stage where the creep rate decreases continuously until it becomes constant, then a short steady creep state exists. It is noticed that, all the creep curves are generally dominated by the primary creep stage and the tertiary creep state is always disappeared. Figure 3 shows a plot of the steady state creep rate,  $\dot{\gamma}^{\circ}$ , against the applied shear stress,  $\tau$ , on a double logarithmic scale. The apparent stress exponent, ( $n_a = \partial \ln \dot{\gamma}^{\circ} / \partial \ln \tau$ ), is not constant and it was found to vary significantly with the applied stress. Two distinctive creep regimes are observed in this graph; low-stress regime and high-stress regime. In low stress regime the apparent stress exponent is  $\sim 3.6$  and in high stress regime its value equals  $\sim 5.5$ . A transition stress is obtained in the region between these two regimes and its value equals  $\sim 3$  MPa. The existence of such a transition stress suggested that a transition from creep driving mechanism to another occurs at this stress<sup>[14]</sup>. The observation of high and variable apparent stress exponent,  $n_a$ , is often attributed to the existence of a threshold stress for creep,  $\tau_0$ <sup>[14, 15]</sup>. On this basis, the observed creep deformation is driven by the effective shear stress,  $\tau_e (= \tau - \tau_0)$  not by the applied stress ( $\tau_0$ ). The rate controlling equation was modified to rationalize the high stress exponent in dispersion strengthened systems and represented by the following equation<sup>[14, 16]</sup>:

$$\dot{\gamma}^{\circ} = A((\tau - \tau_0)/G)^n \exp(-Q/RT) \quad (1)$$

where  $A$  is a constant,  $G$  is the shear stress,  $n$  is the stress exponent,  $Q$  is the apparent activation energy,  $R$  is the gas constant, and  $T$  is the absolute temperature. A procedure was used to estimate  $\tau_0$  from the obtained creep result in which if the creep of this alloy obeys Eq. 1,  $\tau_0$  can be estimated by plotting  $\dot{\gamma}^{\circ 1/n}$  vs  $\tau$  on a double linear scale, where  $n=3, 5, \text{ or } 8$ . Each one of these values represents a particular creep model<sup>[14]</sup>. By extrapolating the resultant straight line to zero creep rate, the corresponding value represents  $\tau_0$ <sup>[15]</sup>. It was found

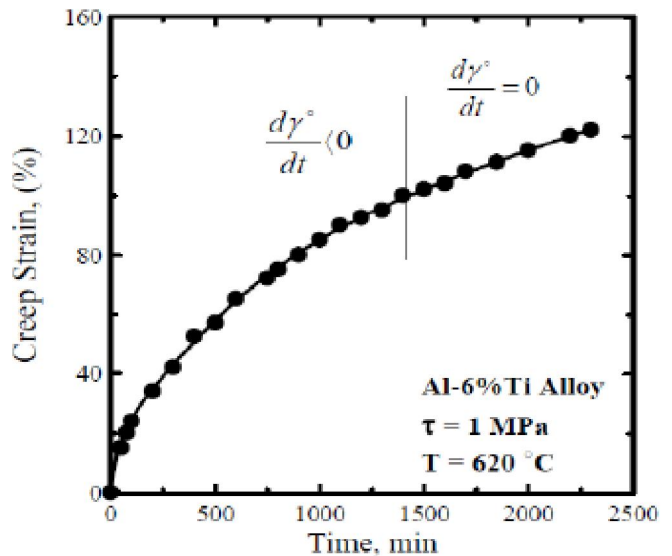


Figure 2 : Typical example of the creep curve of specimen tested under 1 MPa at 620 °C.

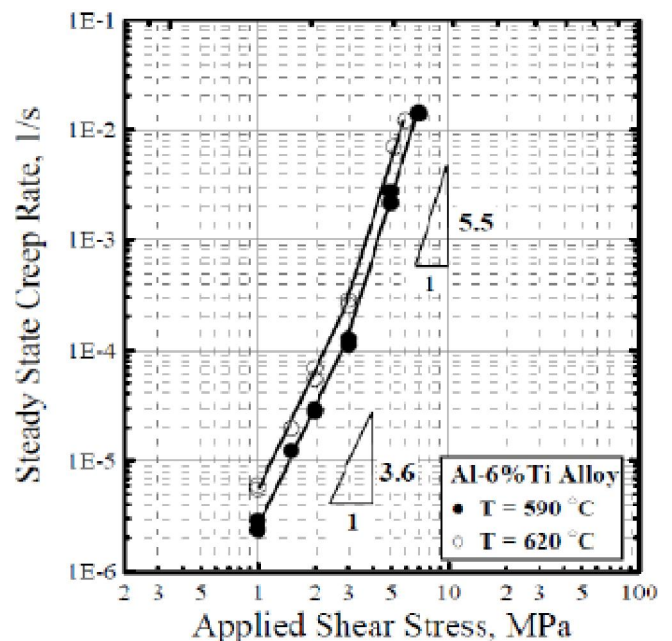


Figure 3 : Steady state creep rate vs applied stress for specimens tested at 590 °C and 620 °C.

## Full Paper

from this procedure that the most appropriate linear fitting is for  $n=5$  and in this case  $\tau_0$  equals to 0.5 MPa. The estimated value of stress exponent,  $n$ , suggests that the present material is creep controlled by high temperature dislocation climb (lattice diffusion) in pure metals<sup>[17]</sup>. These results suggest the present material reached the state of Newtonian viscous deformation in which Newtonian flow control the elevated temperature creep deformation.

### Microstructure observations

Figure 4 shows samples of photomicrographs of Al-6wt.%Ti specimens in the as-cast, after hot extrusion and after creep testing. Two major phases are co-existed; Al matrix and  $Al_3Ti$  intermetallic compound particles in a randomly oriented flaky shape. From Figure 4a it is obvious that the flaky shaped  $Al_3Ti$  is uniformly distributed without any micro-segregations. The average particle size,  $\bar{d}$ , of  $Al_3Ti$  in this case is  $\sim 140 \mu m$ . Figure 4b shows a micrograph of hot extruded Al-6wt.%Ti specimen. It clear that the majority of  $Al_3Ti$  flaks have been fractured into small segments. The distribution of  $Al_3Ti$  phase is inhomogeneous in the Al matrix and its average particle size decreased significantly to be  $\sim 75 \mu m$ . It is obvious that the application of extrusion process to the material affects the distribution of second phase,  $Al_3Ti$ , by breaking them into shorter segments. Figure 4c shows a micrograph of the material after long time annealing and creep testing. Relatively uniform distribution of the  $Al_3Ti$  compound in small size, compared to the other two cases, is observed. It is evident that annealing and creep testing breaks  $Al_3Ti$  particles into smaller segments and redistribute them in regular manner. The average size of  $Al_3Ti$  phase decreased to be  $\sim 67 \mu m$  and the interplaner distance between  $Al_3Ti$  particles decreased from  $95 \mu m$ , for as-cast specimen to be  $35 \mu m$  for the crept one. According to Al-Ti phase diagram<sup>[9]</sup>, the weight fraction of  $Al_3Ti$  compound can be estimated from the content of Ti, by assuming that the element was fully reacted with aluminum to form the  $Al_3Ti$  compound. The calculation showed that the alloy contains  $\sim 25 \text{ wt}\%$   $Al_3Ti$  compound.

A large number of micrographs are used to analyze the features of  $Al_3Ti$  intermetallic compound. Histograms of the distribution of particles size,  $\bar{d}$ , and aspect ratio,

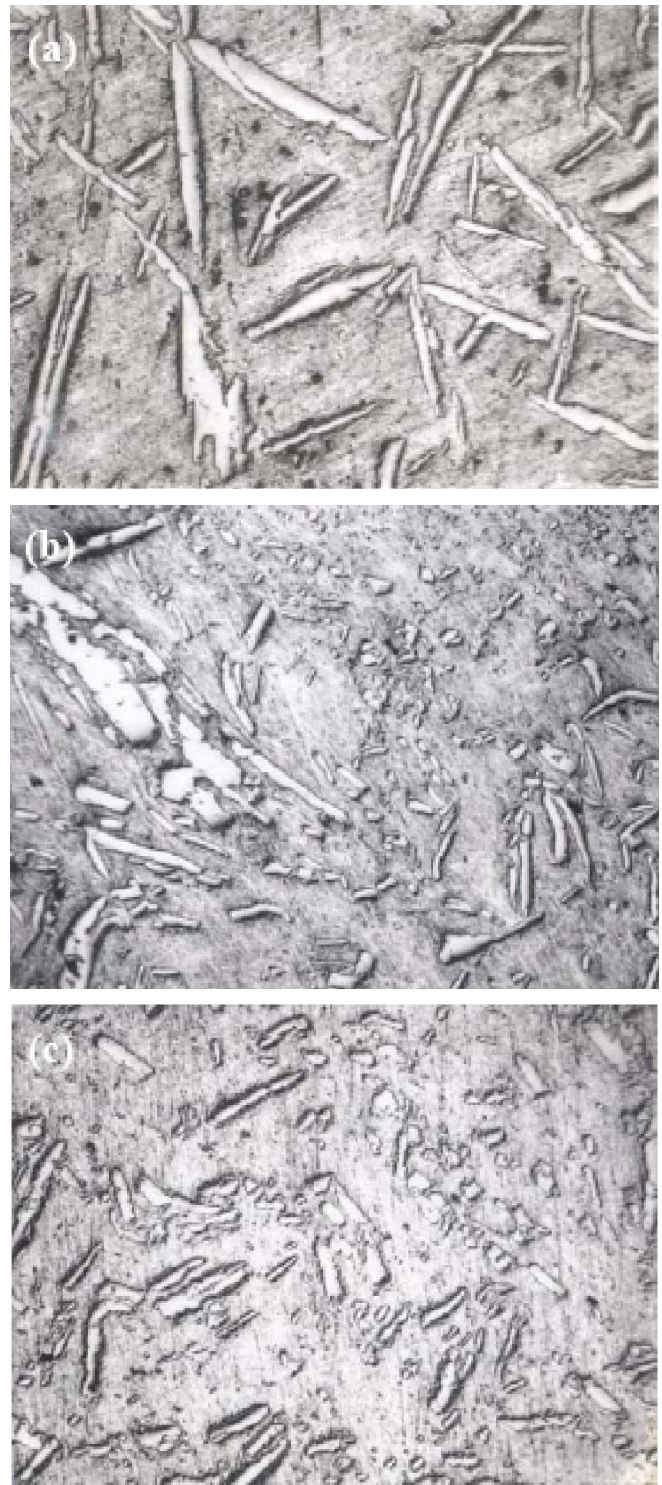


**Figure 4 :** Photomicrographs of Al-6wt.%Ti ally specimens. (X200 for all graphs) Ascast, b) After hot extrusion, and c) after creep test under 1 MPa at 620 °C.

$S=l/d$ , against their count, using image facilities, are shown in Figures 5-7. Generally The distribution is Gaussian for the average particles size and aspect ratio with a confidence limit 95%. As shown in Figure 5a,

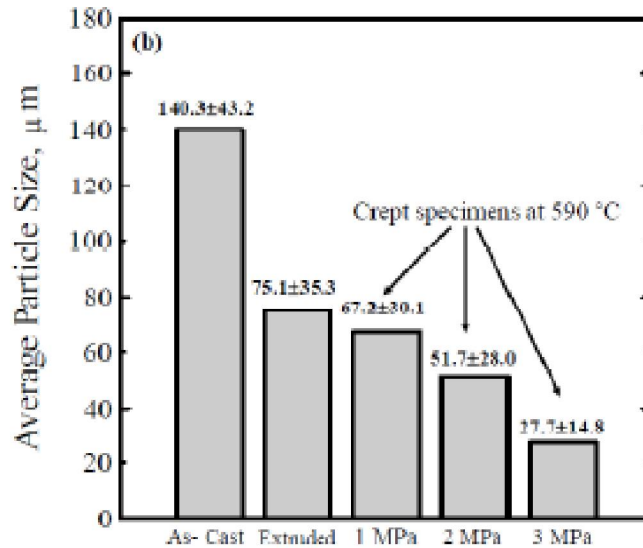
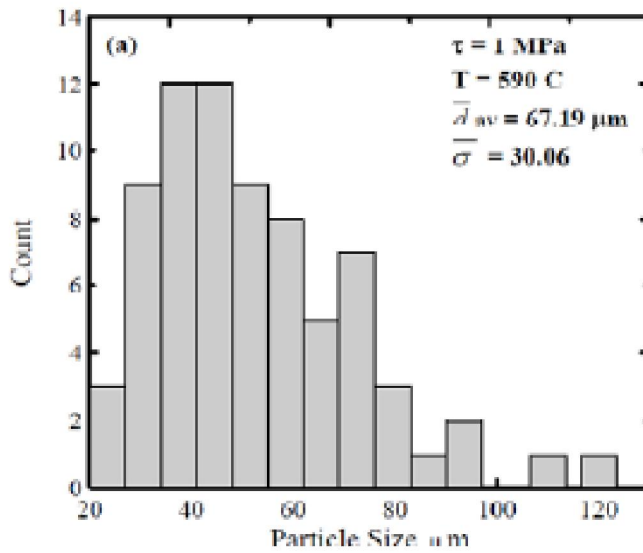


**Figure 5 :** Histograms of Al<sub>3</sub>Ti particle (590 °C); a) typical example for a crept specimen  $\tau=1$  MPa, and b) comparison between different processes.

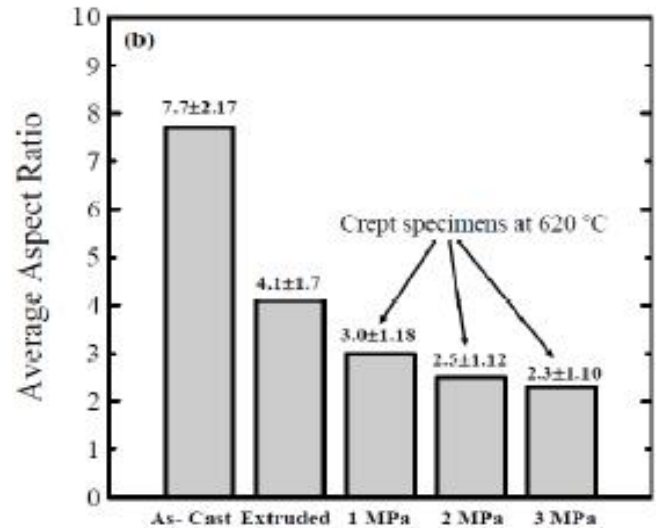
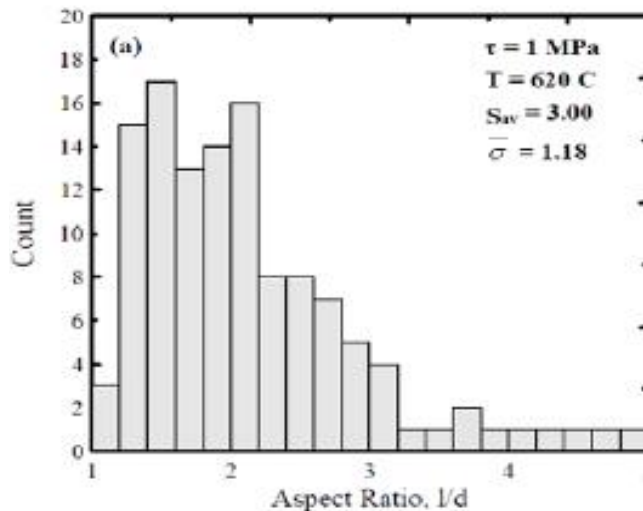


**Figure 6 :** Histograms of Al<sub>3</sub>Ti Aspect (620 °C); a) typical example for a crept specimen  $\tau=1$  MPa, and b) comparison between different processes.

the particles size is inhomogeneous and the maximum relative frequency is close to the average particle size. In Figure 5b significant decrease in the particles size obtained when the as-cast material is hot extruded, this besides the average particle size continue its decrease as the creep stress increased. Figure 6 shows the estimated aspect ratio of Al<sub>3</sub>Ti compound under different processes. It is found that large decrease in the aspect ratio was obtained after the application of hot extrusion process to the as-cast specimens. The average aspect ratio decreased from 7.7 for as-cast samples to 4.1 for hot extruded samples and this decrease continued at elevated temperature creep to be 3. Figure 7 (a and b) represents typical examples of histograms of the aspect ratio of Al<sub>3</sub>Ti compound of the shoulders of crept specimens under 2 MPa and 3 MPa at 590 °C. A close comparison between the two cases shows that there is no significant difference in the aspect ratio for specimens' shoulders. Meanwhile, as shown in Figure 7c, considerable reduction in the aspect ratio is obtained for the gage sections of a crept specimen under 3 MPa compared to that under 2 MPa. The improvement in the features of Al<sub>3</sub>Ti compound suggests that hot extrusion process and creep deformation has a significant role on the grain refinement of the Al<sub>3</sub>Ti intermetallic compound. Microstructural changes experienced by hot extrusion is attributed to the presence of hot working processes that results in large high temperature plastic flow in the matrix material which in turn break the large

## Full Paper

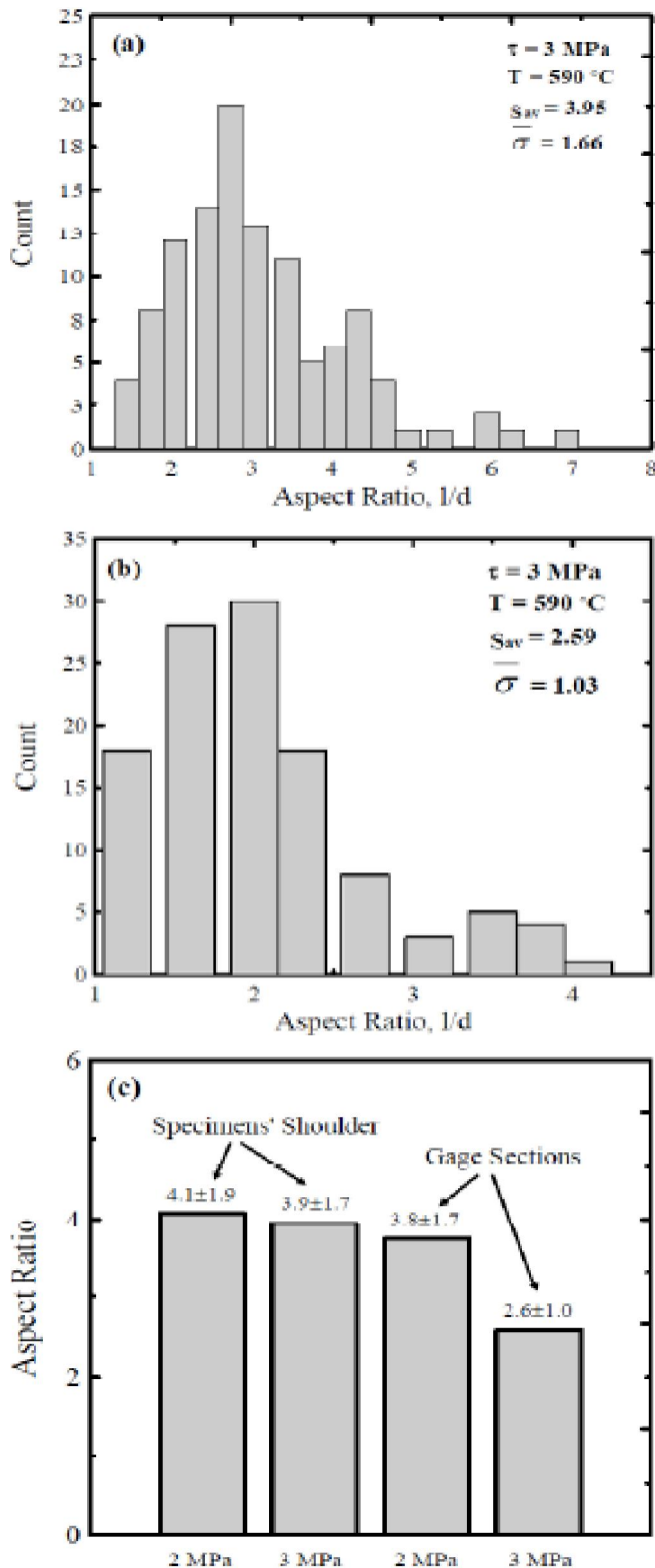


**Figure 7 :** Histograms of the aspect ratio of Al<sub>3</sub>Ti particles (590 °C); a) Sample of histogram of a crept specimen shoulder,  $\tau=3$  MPa, b) Sample of histogram of a crept specimen gage section,  $\tau=3$  MPa, and c) comparison between aspect ratios of shoulders and gage section of two crept specimens under 2 and 3 MPa.

flaky shaped particles to smaller ones. An extra energy is given to the material during high temperature creep deformation that provides a driving force to break and redistribute Al<sub>3</sub>Ti intermetallic compound reaching an improved size and aspect ratio. Additional effort should be paid to investigate the mechanical behavior of this material after the application of these after-fabrication treatments.

## CONCLUSIONS

The microstructure changes of ingot metallurgy Al-6wt.%Ti alloy have been studied, in this paper, under three different states, namely; as-cast, after hot extrusion, and after high temperature creep testing. Based on the preceding experimental results and discussions, the following conclusions can be made.

1. The creep curves are dominated by the primary creep stage followed by a short steady state and the tertiary creep stage always disappeared. The threshold stress appeared here to interpret the observed high values of the stress exponent for creep. The present material exhibited a high stress exponent and its value is not constant along the used stress range.
2. Significant improvements in the features of Al<sub>3</sub>Ti intermetallic compound are obtained after the application of hot extrusion process and elevated temperature creep to the as-cast material. The particle size of Al<sub>3</sub>Ti compound decreased from 140  $\mu$ m, for as-cast material, to 67  $\mu$ m for that subjected to 1 MPa at 590 °C, and this decrease continued, with increasing the creep stresses, up to 27.7  $\mu$ m. Parallel decreases in the aspect ratio of Al<sub>3</sub>Ti compound are obtained with the application of same processes. These results suggested that such processes improves the size and aspect ratio of the large needle shape Al<sub>3</sub>Ti particles to uniformly distributed smaller particles.

## ACKNOWLEDGMENT

The author wishes to acknowledge the materials lab staff and the department of mechanical of engineering at Qassim University, KSA, for providing the materials and their help in running some the experimental work.

**REFERENCES**

- [1] K.M.Lee, I.H.Moon; Mater.Sci.Eng.A., **185**, 165-170 (1994).
- [2] J.H.Choi, K.I.Moon, J.K.Kim, Y.M.Oh, J.H.Suh, S.J.Kim; J.Alloys and Comp., **315**, 178-186 (2001).
- [3] R.J.Arsenault; Key Eng.Mater., **79-80**, 265-278 (1993).
- [4] Q.Xu, V.V.Gupta, E.J.Lavernia; Acta.Mater., **48**, 835-849, (2000).
- [5] J.A.Hawk, P.K.Mirchandani, R.C.Benn, H.G.F.Wisdorf; "Dispersion Strengthened Aluminum Alloys", Edit by Y.W.Kim, W.M.Griffith, 55 (1988).
- [6] P.K.Merchandani, R.C.Benn, H.A.Heck; "Light-Weight Alloys for Aerospace Applications", Edit by E.W.Lee, E.H.Chia, N.J.Kim, TMS-AIME, 33, (1989).
- [7] J.Szajnar, T.Wróbel; J.of Achievements in Mater and Manuf.Eng., **23(1)**, 51-54 (2007).
- [8] L.Xiangfa, Y.Lina, L.Jianwen, W.Zhenqing; Mater.Sci.Eng.A., **399**, 267-270 (2005).
- [9] V.T.Witusiewicz, A.A.Bondar, U.Hecht, S.Rex, T.Ya.Velikanova; J.Alloys and Comp., **465**, 64-77 (2008).
- [10] P.T.Li, X.G.Ma, Y.G.Li, J.F.Nie, X.F.Liu; J.of Alloys and Comp., 1-16 (2010).
- [11] W.Pilarczyk, R.Nowosielski, M.Jodkowski, K.Labisz, H.Krztoń; Archives Mater.Sci.Eng., **31(1)**, 29-32 (2008).
- [12] J.Szajnar, T.Wróbel; J.Achievements in Mater.Manuf.Eng., **23(1)**, 51-54 (2007).
- [13] C.Mayr, G.Eggeler, G.A.Webster, G.Peter; Mater.Sci.Eng.A., **199(2)**, 121-130 (1995).
- [14] A.Abo El-Nasr, F.A.Mohamed, J.C.Earthman; Mater.Sci.Eng.A., **214**, 33-41 (1996).
- [15] C.J.Choi, K.J.Park, W.W.Park; Scripta.Mater., **36(7)**, 769-774 (1997).
- [16] F.A.Mohamed, K.T.Park, E.J.Lavernia; Mater.Sci.and Eng.A., **150**, 21-35 (1992).
- [17] A.Abo El-Nasr, F.A.Mohamed, J.C.Earthman; Mater.Sci.Eng.A., **214(1-2)**, 33-41 (1996).
- [18] O.D.Sherby, G.Gonzalez-Doncel, O.A.Ruano; "Threshold Stresses in Particle-Hardened Materials", in Creep and Fracture of Engineering Materials and Structures, J.C.Earthman and F.A.Mohamed (Eds.), The Minerals, Metals & Materials Society, Warrendale, PA, 9-18 (1997).
- [19] K.T.Park, E.J.Lavernia, F.A.Mohamed; Acta.Metall.Mater., **38(11)**, 2149-2159 (1990).